Culture of equine fibroblast-like synoviocytes on synthetic tissue scaffolds towards meniscal tissue engineering: a preliminary cell- seeding study

Introduction: Tissue Engineering is a new methodology for addressing meniscal injury or loss. Synovium may be an ideal source of cells for *in vitro* meniscal fibrocartilage formation, however, favorable *in vitro* culture conditions for synovium must be established in order to achieve this goal. The objective of this study was to determine cellularity, cell distribution, and extracellular matrix (ECM) formation of equine fibroblast-like synoviocytes (FLS) cultured on synthetic scaffolds, for potential application in synovium-based meniscal tissue engineering. Scaffolds included open-cell poly-L-lactic acid (OPLA) sponges and polyglycolic acid (PGA) scaffolds cultured in static and dynamic culture conditions, and PGA scaffolds coated in poly-L-lactic (PLLA) in dynamic culture conditions. **Materials and Methods:** Equine FLS were seeded on OPLA and PGA scaffolds, and cultured in a static environment or in a rotating bioreactor for 12 days. Equine FLS were also seeded on PGA scaffolds coated in 2% or 4% PLLA and cultured in a rotating bioreactor for 14 and 21 days. Three scaffolds from each group were fixed, sectioned and stained with Masson's Trichrome, Safranin-O, and Hematoxylin and Eosin, and cell numbers and distribution were analyzed using computer image analysis. Three PGA and OPLA scaffolds from each culture condition were also analyzed for extracellular matrix (ECM) production via dimethylmethylene blue (sulfated glycosaminoglycan) assay and hydroxyproline (collagen) assay. PLLA coated PGA scaffolds were analyzed using double stranded DNA quantification as areflection of cellularity and confocal laser microscopy in a fluorescent cell viability assay. **Results:** The highest cellularity occurred in PGA constructs cultured in a rotating bioreactor, which also had a mean sulfated glycosaminoglycan content of 22.3μg per scaffold. PGA constructs cultured in static conditions had the lowest cellularity. Cells had difficulty adhering to OPLA and the PLLA coating of PGA scaffolds; cellularity was inversely proportional to the concentration of PLLA used. PLLA coating did not prevent dissolution of the PGA scaffolds. All cell scaffold types and culture conditions produced non-uniform cellular distribution. **Discussion/ Conclusion:** FLS-seeding of PGA scaffolds cultured in a rotating bioreactor resulted in the most optimal cell and matrix characteristics seen in this study. Cells grew only in the pores of the OPLA sponge, and could not adhere to the PLLA coating of PGA scaffold, due to the hydrophobic property of PLA. While PGA culture in a bioreactor produced measureable GAG, no culture technique produced visible collagen. For this reason, and due to the dissolution of PGA scaffolds, the culture conditions and scaffolds described here are not recommended for inducing fibrochondrogenesis in equine FLS for meniscal tissue engineering.

Culture of equine fibroblast-like synoviocytes on synthetic tissue scaffolds towards meniscal tissue engineering: a preliminary cell- seeding study

1) Jennifer J. Warnock, Comparative Orthopaedic Laboratory, University of Missouri, Columbia, MO; Dr. Warnock's current address is College of Veterinary Medicine, Oregon State University, Corvallis OR
2) Derek B. Fox, Comparative Orthopaedic Laboratory, University of Missouri, Columbia, MO;
3) Aaron M. Stoker, Comparative Orthopaedic Laboratory, University of Missouri, Columbia, MO
4) Mark Beatty, VA Nebraska-Western Iowa Health Care System and University of Nebraska Medical Center College of Dentistry, Lincoln, NE
5) Mary Cockrell, Comparative Orthopaedic Laboratory, University of Missouri, Columbia, MO
6) John C. Janicek, Comparative Orthopaedic Laboratory, University of Missouri, Columbia, MO
7) James L. Cook, Comparative Orthopaedic Laboratory, University of Missouri, Columbia, MO

This study was funded by the Comparative Orthopaedic Laboratory, University of Missouri, Columbia, MO 65211

,

CORRESPONDING AUTHOR:
Jennifer J. Warnock,
Dr. Warnock's current address is:
Magruder Hall, College of Veterinary Medicine
Oregon State University, Corvallis OR 97331
541-737-4812
jennifer.warnock@oregonstate.edu

Dr. Janicek's current address is
Brazos Valley Equine Hospital
Navasota, TX 77868

Introduction:

The knee menisci are semilunar-shaped fibrocartilages with extracellular matrix (ECM) composed primarily of types I and II collagen, glycosaminoglycans (GAGs), and water (Fithian et al. 1990). It is now well established that intact menisci are crucial for the maintenance of normal joint function, however these critical structures are frequently injured in humans and animals. Meniscal tears are the most common knee injury in people, and arthroscopic meniscectomy represents the most common human orthopedic surgery performed annually (Burks et al. 1997). Meniscal injuries are also a significant cause of lameness and decreased performance in horses (Peroni & Stick 2002; Walmsley 1995; Walmsley et al. 2003); equines affected by naturally occurring meniscal tears may also be a viable model for the study of human meniscal injury.

As the axial, avascular portion of the meniscus has a limited ability to heal spontaneously, (Arnoczky & Warren 1983; Kobayashi et al. 2004), the majority of meniscal injuries are treated with partial menisectomy. However, this also results in eventual articular cartilage damage of the tibia and femoral condyles, and progression of debilitating osteoarthritis (Arnoczky & Warren 1983; Cox et al. 1975). Thus tissue engineering new meniscal fibrocartilage is being investigated as a treatment for avascular meniscal injuries.

Synovium may be an ideal cell source for meniscal tissue engineering. Synovium plays an important role in attempted vascular zone healing and regeneration (Cisa et al. 1995; Kobuna et al. 1995; Ochi et al. 1996; Shirakura et al. 1997). Synovium has the ability to form fibrocartilaginous-like tissue *in vivo* in response to meniscectomy (Cox et al. 1975). In addition, synoviocytes have been reported to be an important element in cellular repopulation of meniscal allografts (Arnoczky & Warren 1983; Rodeo et al. 2000). Synovial tissue progenitor cells, grossly indistinguishable in culture from type B or fibroblast-like synoviocytes (FLS), can undergo chondrogenesis *in vitro* (De Bari et al. 2001; Nishimura et al. 1999). Taken together, these data

indicate that synovium may be able to serve as a source for functional fibrocartilage in engineering meniscal tissue, provided the chondrogenic potential of synoviocytes can be optimized.

Tissue engineering scaffolds must provide substrate and stability for cellular retention, intercellular communication, and cellular growth to allow seeded cells to proliferate extracellular matrix (ECM). As the scaffolds naturally degrade, the cellular ECM must be able to take on the biomechanical function and form previously designated by the scaffolds to maintain construct integrity. Thus a scaffold must be hydrophilic enough to allow cell adhesion but have a long enough half- life to not prematurely dissolve, which would prevent ECM proliferation and cell death. PGA (poly -glycolic acid) and PLA (poly-L- lactic acid) are biodegradable, biocompatible, poly-esters, that are attractive for tissue engineering because they are readily available, can be easily processed into a variety of structures, and are approved by the Food and Drug Administration for a number of biomedical applications (Lavik et al. 2002). PGA has been successfully used as a scaffold for meniscal fibrochondrocytes *in vivo* (Kang et al. 2006) and cultured *in vitro* (Aufderheide & Athanasiou 2005) to form meniscal-like tissue. Another scaffold type, PLLA, (poly-L lactic acid) has been successfully used for *in vitro* tissue engineering of leporine meniscal fibrochondrocytes (Esposito et al. 2013; Gunja & Athanasiou 2010), chondrocytes (Sherwood et al. 2002), and human fibroblasts (Hee et al. 2006). PGA –PLLA combinations have also been successfully used for *in vitro* meniscal culture (Ionescu & Mauck 2013). In addition, chondrocytes cultured on PGA-PLLA mixtures versus collagen sheets contain more collagen type II and have stronger mechanical properties (Beatty et al. 2002) than single polymer scaffolds. Further investigation of combination use of PLLA combined with PGA for *in vitro* synoviocyte culture is warranted.

Cartilage and fibrocartilage engineering with biodegradable scaffolds is most successful if uniform cell distribution is achieved (Davisson et al. 1999; Pazzano et al. 2000; Smith et al.

1995), which is optimized through the use of rotating bioreactors(Aufderheide & Athanasiou 2005; Kim et al. 1998; Pazzano et al. 2000). In addition, rotating bioreactors provide mechanical stimulation of cultured cells. This has a positive effects on cell differentiation, cell viability, extracellular matrix production, and compressive biomechanical properties, through mechanotransductive effects (Davisson et al. 1999; Imler et al. 2004; Pazzano et al. 2000; Smith et al. 1995). Thus scaffold culture in a rotating bioreactor may represent a useful technique for synoviocyte- based engineering of functional meniscal tissue.

Based on this prior research, we believe that both PGA and PLLA would be viable synthetic scaffolds for the *in vitro* culture of FLS for application in meniscal fibrocartilage tissue engineering. Thus, the first objective of this study was to 1) determine cell distribution and ECM formation of equine FLS seeded and cultured dynamically in a rotating bioreactor versus static seeding and culture, on two synthetic scaffold types, PGA and open- cell PLLA (OPLA). The second objective was to compare cell viability, distribution, and ECM formation of FLS cultured on 2% vs 4% PLLA coated PGA scaffolds, cultured for 14 or 21 days. Our hypothesis was that we would see no difference in equine FLS content, FLS distribution, and ECM formation between scaffold type, biomechanical culture environment, and culture duration.

Materials and Methods:

Experiment 1:

*Tissue Collection and Monolayer Cell Culture***--** Six 8.0 mm x 8.0 mm biopsies of synovial intima and subintima were obtained from both stifles of an adult American Quarter Horse, euthanatized according the American Veterinary Medical Association's guidelines for humane euthanasia, for reasons unrelated to the study. The horse was determined to be free of orthopedic disease based on pre-mortem physical examination and post mortem gross examination of the joint. Tissue was placed in Dulbeccos' Modified Eagle's Media (DMEM) with 10% fetal bovine serum, 0.008% Hepe's buffer, 0.008% non-essential amino acids, 0.002%

penicillin 100I.U./mL streptomycin 100ug/mL, amphoterocin B 25ug/mL, 0.002% L-ascorbate, and 0.01% L-glutamine in preparation for monolayer culture.

Synovium was sectioned into 2.0mm x 2.0mm pieces using a #10 Bard Parker blade under sterile conditions. The tissue fragments were combined with sterile Type 1A clostridial collagenase solution (Type 1A Clostridial Collagenase, Sigma, St. Louis, MO) at a concentration of 7.5mg/mL of RPMI 1640 solution. The mixture was agitated at 37˚C, 5% CO2, 95% humidity for six hours. Cells were recovered through centrifugation, the supernatant decanted and the cellular pellet re-suspended in 5mL of supplemented DMEM. The cell solution was transferred to a 25cm^2 tissue culture flask containing 5mL of supplemented DMEM. The flasks were incubated at 37˚C, 5% CO2, 95% humidity, with sterile medium change performed every 3 days. Synovial cells were monitored for growth using an inverted microscope until observance of 95% cellular confluence per tissue culture flask. At second passage cells were transferred to 75cm^2 tissue culture flasks containing 11mL of media. At 95% confluence the cells were subcultured until the 4th cell passage had been reached. At 4th passage cells were removed from flasks, counted using the Trypan Blue exclusion assay (Strober 2001), and transferred to scaffold culture as described below.

Scaffolds—A non- woven polyglycolic acid (PGA, Tissue Scaffold, Synthecon, Houston, TX) felt, 3mm thick, with 10µm diameter fibers was utilized for this study. The open-cell poly-lactic acid (OPLA sponge, BD Biosciences, Bedford, MA) utilized were 5.0mmx 3.0mm, non compressible, cylindrical sponges. The average OPLA sponge pore size was 100-200µm with a hydration capacity of 30µl/ scaffold. PGA and OPLA scaffolds were sterilized in ethylene oxide. Following sterilization, the PGA felt was cut using a sterile Baker's biopsy punch to create into 5.0mm x 3.0mm discs prior to cell culture to match the dimensions of the OPLA scaffolds.

Dynamic Culture-- Twelve PGA scaffolds (PGA-D group) and 12 OPLA sponges (OPLA-D group) were placed in separate 110mL vessel flasks of a rotating bioreactor system (Rotating

Bioreactor System, Synthecon, Houston, TX (Fig. 1) containing 110mL of supplemented DMEM. The scaffolds were presoaked for 24 hours in the bioreactor at 37˚C, 5% CO2, 95% humidity, prior to cell introduction. Fourth passage FLS were removed from the tissue culture flasks enzymatically (Accutase Innovative Cell Technologies, San Diego, CA) and counted. Cells were added to the 110mL bioreactor flasks at a concentration of 1 million cells/ scaffold via a 60cc syringe, slowly injected over several minutes. For the duration of the study the bioreactor vessels were rotated at 51.1 rpm to allow the scaffolds to free-float and rotate within the culture medium, without contacting the inner bioreactor surfaces. Cultures were maintained at 37˚C, 5% CO2, 95% humidity. Fifty percent of the cell culture medium volume was changed using sterile technique every 3 days. Cell counts were performed on discarded media for the first two media changes.

Static Culture-- Twelve PGA scaffolds (PGA-S group) and 12 OPLA sponges (OPLA-S group) were placed individually in non- treated 24 well tissue culture plates, each well containing 2mL of supplemented DMEM (Fig. 2). The scaffolds were presoaked for 24 hours at 37˚C, 5% CO2, 95% humidity, prior to cell introduction. Then FLS were transferred from monolayer culture as described above, and slowly over 3 minutes, pipetted on top of the scaffolds in solution, at 1 million cells per scaffold in each well. The plates were maintained at 37˚C, 5% CO2, 95% humidity, with 50% cell culture medium changed every 3 days. Cell counts were performed on discarded media for the first 2 media changes.

Histologic Analysis-- All scaffolds were harvested on the 12th day of culture. Six scaffolds from each group (PGA-S, PGA-D, OPLA-S, OPLA-D) were fixed in 10% buffered formalin, embedded in paraffin, sectioned, and stained with Masson's Trichrome, Safranin –O, and Hematoxylin and Eosin. Histologic specimens were examined at 10x magnification (Zeiss Microscope, Carl Zeiss, Thornwood, NY). Images of each section, (three from the scaffold periphery and three from the scaffold center) at 2 o'clock, 6o'clock and 10o'clock positions (Fig.

3) were digitally captured by a digital camera (Olympus DP-70 Olympus, Melville, NY) and saved as tagged- image file format images. Digital image analysis was performed as previously validated (Amin et al. 2000; Benzinou et al. 2005; Girman et al. 2003; Goedkoop et al. 2005) whereby cellular density was assessed using a thresholding algorithm (Loukas et al. 2003) using computer image analysis (Fovea 3.0, Reindeer Graphics, Asheville, NC). This algorithm allows quantification of cellular nuclei based on their histogram values. All cell counts were additionally validated by hand counts. Safranin-O staining, indicating presence of GAG, and Masson's Trichrome staining, indicating presence of collagen, were subjectively evaluated and recorded.

Biochemical ECM Analysis-- Three cultured scaffolds from each group were analyzed for glycosaminoglycan (GAG) and collagen production. Wet weight of each scaffold was obtained. GAG content of the scaffold was performed using the Dimethyl-methylene Blue Sulfated Glycosaminoglycan assay (Farndale et al. 1986). Collagen content of the cultured scaffolds was assessed using the hydroxyproline assay, as described by Reddy et al.(Reddy & Enwemeka 1996).

Statistical Methods—Data were tested for normality using a Shapiro-Wilk test. Data were then analyzed using a one way analysis of variance followed by a Tukey's test, to compare the effect of scaffold type and seeding technique on cell counts and ECM quantity. To determine significance between periphery and central cell counts within each scaffold, a paired, 2-tailed student's t-test was performed. For all tests significance was set at $P < 0.05$. All statistical analyses were performed using a statistical software program, (GraphPad Prism Version 6, San Diego, CA).

.

Experiment 2:

Scaffolds-- PLLA was dissolved in methylene chloride as a 2% or 4% solution. The 2% and 4% PLLA solution each was applied to a 3.0 mm thick sheet of the same, above- described, non- woven PGA felt, using an eye-dropper. Following PLLA treatment, the treated felt was placed in a vacuum dessicator overnight and then sterilized in ethylene oxide. Following sterilization, the 2% and 4% PLLA modified PGA felts were cut into fourteen 5mmx 7mmx 3mm square scaffolds using sterile scissors and a #10 bard parker blade (Fig 4).

Tissue Collection and Monolayer Cell Culture **--** Synovial intima/ subintima was harvested from the stifles of two mixed breed, adult horses euthanatized according the American Veterinary Medical Association's guidelines for humane euthanasia, for reasons unrelated to the study. These horses were also determined to be free of orthopedic disease based on pre-mortem physical examination and post mortem gross examination of the joint. The tissue was transported, minced and digested as described above. Cells were recovered through centrifugation, the supernatant decanted and the cellular pellet re-suspended in 5mL of supplemented DMEM. The cell solution was transferred to a 25mL tissue culture flask containing 5mL of supplemented DMEM. Cells were grown in monolayer culture, under the conditions described above, until the 4^{th} cell passage had been reached.

Dynamic Culture-- Fourteen 2% PLLA coated PGA scaffolds and fourteen 4% PLLA coated PGA scaffolds were placed in separate 110mL vessel flasks of the rotating bioreactor system containing 110mL of supplemented DMEM. The scaffolds were presoaked for 24 hours in the bioreactor at 37˚C, 5% CO2, 95% humidity, prior to cell introduction. After this time it was noted that the scaffolds were floating at the apex of the flasks. Using sterile surgical technique, scaffolds were sterily removed from the flasks, pierced centrally, and strung on loops of 3-0 nylon surgical suture with knots placed adjacent to the scaffolds to prevent bunching on the line. Seven scaffolds were placed per suture. The strings of scaffolds were then placed back in to the

bioreactors and presoaked for another 12 hours, at which time complete hydration and submersion were achieved (Fig. 5).

Scaffolds were then dynamically seeded. Synovial membrane cells were removed from the tissue culture flasks using as described above and counted using the Trypan Blue exclusion assay (Strober 2001). Cells were added to the bioreactor flasks at a concentration of 475,000 cells per mL.

For the duration of culture, the bioreactor was maintained at 37˚C, 5% CO2, 95% humidity at 51.1 rpm. Fifty percent of the cell culture medium volume was changed using sterile technique every 3 days. Seven scaffolds were harvested on day 10 of culture, and 7 scaffolds were harvested on day 21 of culture.

Determination of Cell Viability-- Cell viability was determined with the use of ethidium homodimer-1 (4ul/ml PBS) and Calcein AM (Acetoxymethylester) (0.4ul/ml PBS) fluorescent stains (Invitrogen, Carlsbad CA) and the use of Confocal Laser Microscopy. The Confocal Laser Microscope consists of the BioRad Radiance 2000 confocal system coupled to an inverted microscope (Olympus IX70 Olympus, Melville, NY) equipped with Krypton-Argon and red diode laser. Approximately 1.0 mm sections were made from the halved scaffold using a rotary paper cutter. A section from each scaffold's cut center and a section from each scaffold's periphery was examined. Sections were incubated with the staining agents for 30 minutes at room temperature, placed on a glass microscope slide, moistened with several drops of PBS, and stained using the fluorescent double labeling technique. The sections were examined under 10x magnification. Images were taken of each specimen as described above, (three from the section periphery and three from the section center) at the 2 o'clock, 6o'clock and 10o'clock positions. Images were digitally captured as described above. Live and dead cell counts were determined by hand counts.

DNA Quantification -- One half of each construct was lyophilized and a dry weight obtained. Samples were incubated in 1.0ml Papain Solution (2mM Dithiothreitol and 300ug/ml Papain) at 60ºC in a water bath for 12 hours. A double stranded DNA quantification assay (Quant-iT PicoGreen™ Invitrogen, Carlsbad, CA) was performed. Double stranded DNA extracted from bovine thymus was mixed with TE buffer (Invitrogen, Carlsbad, CA) to create standard DNA concentrations of 1,000, 100, 10, and 1 ng/mL. The standards and 100uL of each papain digested sample (used in the above GAG and hydroxyproline assays) were added to a black 96 well plate. 100uL of 2ug/mL of Pico Green reagent was added to each well and the plate was incubated for 5 minutes. Sample fluorescence was read at 485nm excitation/ 528nm emission by a spectrophotometric plate reader (Synergy HT – KC-4, BioTek, Winooski, VT). Absorbances were converted to ng/mL concentrations and total double stranded DNA yield in ng using FT4 software (BioTek, Winooski, VT).

Statistical Methods— Data were tested for normality using a Shapiro-Wilk test. Scaffold weights were compared using a 2-tailed paired t-test. Scaffold dsDNA content was analyzed using a repeated- measures analysis of variance with a Geisser-Greenhouse correction. Significance was set at $p < 0.05$. All statistical analyses were performed using a statistical software program, (GraphPad Prism Version 6, San Diego, CA).

Results

Experiment 1:

As determined by the Trypan Blue exclusion assay, viability of cells at the time of transfer from monolayer culture to static or dynamic seeding was 98.6%. No live cells were detected in any of the media changes for either static or dynamically cultured scaffolds, indicating that viable cells rapidly adhered to the scaffolds.

At the time of harvest upon gross examination, the fibers of the PGA scaffolds and the sponge surface of the OPLA scaffolds were still visible. PGA scaffolds subjectively appeared more translucent.

Despite equal cell seeding concentrations, the effect of dynamic bioreactor culture on cell content of PGA scaffolds (PGA-D versus PGA-S) was to increase scaffold cellularity ($P<0.001$). This was also found in OPLA-D versus OPLA-S scaffolds ($P=0.028$). The effect of scaffold type also significantly increased scaffold cellularity of PGA-D versus OPLA-D ($P=0.017$), while OPLA-S had great cellularity than PGA-S ($P=0.0217$; Table 1).

All groups, with the exception of OPLA-S, showed increased cellular distribution to the periphery of the scaffolds (Table 2). Due to the shape of the OPLA-S on histological sectioning, there was overlap of central and peripheral fields of view, precluding accurately localized cell counts; peripheral cell count was 307 ±52 and central cell count was 287 ± 80 ($P<0.464$). Cells grew in whorls, strands, and sheets on the PGA scaffolds, while cells grew in clumps on the surface pores of the OPLA sponges (Fig. 6).

Staining for collagen and gycosaminoglycan using Masson's Trichrome and Safranin-O, respectively, was negative for extracellular matrix production in all sections of all scaffold types and culture conditions evaluated.

In the PGA-D group, the dimethylmethylene blue assay detected a mean of 22.29 μg of GAG per scaffold, (range 19.34- 28.13μg), with a mean % GAG scaffold content of 0.0345% (μg GAG per μg scaffold wet weight). No GAG was detected in OPLA constructs or PGA-S constructs. The hydroxyproline assay did not detect collagen production in any group.

Experiment 2:

Post PLLA modification, mean scaffold dry weights before soaking and seeding were 1.01mg for 2% PLLA coating and 1.52mg for 4% PLLA coating ($P<0.001$). Scaffold dry weights

decreased over time. Mean lyophilized weight on day 10 for 2% PLLA coating was 0.533mg, which decreased to 0.257mg on day 21 (P=0.02). Mean lyophilized weight on day 10 for 4% PLLA coating was 0.481mg, which decreased to 0.381mg on day 21 (P=0.043).

Scaffold cellularity as measured by dsDNA content increased over time: for the 2% group, day 10 cellularity was 102.6 ng dsDNA/mg dry weight, and on day 21 it was 281.79 (P=0.021). On day 10 for the 4% group, dsDNA content was 111.01 ng dsDNA/mg dry weight and on day 21 it was 140.2ng dsDNA/mg dry weight (P= 0.032; Fig. 7).

PLLA coating also affected scaffold dsDNA content. Scaffolds with the 2% PLLA coating had greater dsDNA content than the 4% PLLA coating on day 21 (P=0.003), but not on day 10 (P=0.602; Fig 7).

As visible under confocal microscopy, cells only adhered to the surface of exposed PGA fibers and had poor to no penetration to the scaffold centers in all PLLA coated scaffolds. Viable cell numbers were estimated only because of the marked cellular clumping; all scaffolds showed mixtures of viable and non- viable cells localized in clumps on the scaffold outer margins (Figs 8-11). Histologic examination of H+E stained constructs revealed minimal cellular adhesion to the PLLA, in all groups at all times, with cells growing primarily on the exposed PGA scaffold, in tightly packed clumps, or adhering to exposed fibers of PGA. No extracellular matrix was observed in any scaffolds on histologic analysis, which also reflected the uneven cellularity (Fig 12).

Discussion:

The current study analyzed the effect of scaffold type, biomechanical stimuli, and culture duration on FLS seeding and production of specific meniscal ECM constituents. We found that FLS-seeded PGA constructs cultured in a rotating bioreactor had the highest cellularity, with a mean sulfated glycosaminoglycan content of 22.3μg per scaffold. PGA constructs cultured in

static conditions had the lowest cellularity. For PLLA coated PGA, increasing concentration of PLLA decreased scaffold cellularity, while increased culture time increased scaffold cellularity, as determined by the dsDNA assay. A non-uniform cellular distribution was observed for all scaffold types and culture conditions.

Bioreactor culture provides a number of benefits over static culture, which would account for the higher cellularity of PGA-D and OPLA-D versus PGA-S and OPLA-S scaffolds. The rotating wall bioreactor used in this study provided a dynamic, laminar fluid shear, which perfuses scaffold cultured cells (Bilodeau & Mantovani 2006), and thereby encourages cell survival and proliferation by providing efficient transport of nutrients, gases, catabolites, and metabolites and maintaining physiologic media pH (Gooch et al. 2001; Vunjak-Novakovic et al. 1998). Mixing of culture media also promotes cell seeding by creating matched relative velocities of cells and scaffolds, particularly on non-woven PGA scaffolds (Vunjak-Novakovic et al. 1998). In addition, the rotating wall bioreactor limits cellular stress by reducing strong shear forces and cellular impact on the walls of the bioreactor (Bilodeau & Mantovani 2006). However, in our study, scaffold characteristics such as scaffold density and hydrophilicity may have negated the advantages of bioreactor culture, as seen with OPLA or PLLA coated scaffolds, which had fewer cells and markedly uneven cell distribution, respectively.

A higher cell count was found on PGA-D versus OPLA-D, indicating either better adherence or cell proliferation on PGA. Non-woven PGA scaffolds favor cellular capture and retention because of their polar surface properties and high surface area for cellular adhesion (Day et al. 2004; Moran et al. 2003). Cellularity of PGA-D was further increased by the open weave and low density (45-77mg/cc) of PGA scaffolds supports cellular proliferation through superior flow-through of culture media and nutrient delivery (Vunjak-Novakovic et al. 1998). This is in contrast to the highly dense (871mg/cc) OPLA sponges with non-communicating pores, which could inhibit nutrient and gas transfer to seeded cells (Pazzano et al. 2004; Pazzano et al. 2000; Wu et

al. 1999). For PLLA covered PGA scaffolds, cells were located primarily on exposed PGA fibers, and scaffold cellularity was inversely proportional to the concentration of PLLA. Although PLLA is widely used in tissue-engineering applications because of its slower degradation characteristics, strength, and mechanical properties, its hydrophobic, inert nature can affect cell-matrix interactions and decrease cellular adhesion (Moran et al. 2003). While the PLLA coating of PGA scaffolds was intended to protect from premature scaffold dissolution, we observed that with longer duration of culture, scaffolds appeared to be more fragile to disruption with forceps manipulation, particularly on the outer edges as well as around the centrally placed suture. In agreement with this observation, all scaffold dry weights dropped over time, indicating scaffold dissolution. Thus PLLA did not prevent PGA hydrolysis and decreased scaffold integrity. PLLA coating also provided a hydrophobic barrier to centralized cell seeding and ingrowth. Thus, for the future study of scaffold seeded equine FLS, use of PLLA type scaffolds is not recommended.

Cell distribution across all scaffolds was uneven, in contrast to previous reports on bioreactor chondrocyte culture (Mahmoudifar et al. 2005; Pazzano et al. 2004). Lower central cell density in our scaffolds may have indicated poor axial cell penetration and in-growth. Alternatively, higher peripheral cellularity could reflect increased peripheral cell division caused by increased exposure to media nutrients, gas exchange, and mechanotransductive effects (Mahmoudifar et al. 2002). Additionally the OPLA scaffolds had clumped cell distribution in the outermost pores. The OPLA sponge porosity may not allow uniform cell distribution; the 100-200μm pores do not consistently communicate with each other. While OPLA-S did not have different peripheral and central cell counts, this was due to an artifact of the sponge shape and precluded distinction of peripheral cells from central cells. To increase central scaffold cell content, flow-through bioreactors (Bilodeau & Mantovani 2006) may have greater cell seeding efficiencies than rotary bioreactors. Alternatively, cells may be seeded at the time of scaffold formation, such as during hydrogel synthesis, to insure central scaffold cellularity (Narita et al. 2009).

The culture conditions utilized in the present study resulted in minimal to no ECM formation, in contrast to other studies. The mean GAG content of the PGA-D scaffold of 0.0345% (wet weight basis) was lower than the 0.6-0.8% wet weight in the normal meniscus, and thus represents a sub- optimal response for engineering purposes (AufderHeide & Athanasiou 2004). Synoviocytes typically produce collagen type I constitutively, (Garner & al. 2000; Levick 1996), however production and deposition of hydroxyproline was not detected in this study. The most likely reason for this failure of ECM formation was lack of culture with a specific fibrochondrogenic media. For example, culture with recombinant transforming growth factor-beta, insulin-like growth factor -1 and basic fibroblast growth factor have been shown to induce *in vitro* collagen formation in human synoviocytes (Pei et al. 2008). Treatment of equine FLS with recombinant chondrogenic growth factors, in addition to the scaffold and bioreactor culture conditions used in the present study, resulted in greater type II collagen and aggrecan gene expression (Fox et al. 20010).Reported scaffold seeding concentrations for cartilage tissue engineering include 30,000 fibroblasts/mL (Day et al. 2004); 600,000 chondrocytes/mL (Stading M & R 1999); 5 million chondrocytes/ mL (Griffon et al. 2005); and 10 million chondrocytes/mL (Hu et al. 2005). Our seeding density of 1 million equine FLS per scaffold may have been too low, as dense cell aggregates are required for meniscal developmental fibrochondrogenesis (Clark & Ogden 1983) due to the embryonic community effect (Gurdon et al. 1993). In the present study the FLS were exposed to the mild shear forces and hydrostatic pressurization in a rotating bioreactor (Mauck et al. 2002) which may not have been the optimal type of forces required for synovial collagen I formation. A combination of in vitro tensile and compressive forces(AufderHeide & Athanasiou 2004; Benjamin & Ralphs 1998) may be required to support formation GAG (Valiyaveettil et al. 2005) and types I and II collagen (Kambic & McDevitt 2005), the major ECM components of fibrocartilage. Cell culture on scaffolds may also result in cellular stress shielding, thereby resulting in suboptimal matrix formation (Huey & Athanasiou

2011). Synovial macrophages may have contaminated our FLS cultures, thereby also decreasing ECM formation (Pei et al. 2008, Bilgen et al. 2009) and future studies should include negative isolation of macrophages. Additionally, co-culture with meniscal fibrochondrocytes as decribed by Tan and workers (Tan et al. 2010) may have also helped fibrochondrogenic differentiation of equine FLS and will be the focus of future studies. Increased culture time may also be beneficial to ECM formation; other studies show time dependent ECM expression (Griffon et al. 2005; Mueller et al. 1999; Sha'ban et al. 2008). One study of synovial chondrogenesis on PGA scaffolds utilized a longer culture duration of 60 days, with successful ECM formation (Sakimura et al. 2006). Despite better cellularity, PGA scaffolds began loosing integrity over the culture period, even when coated with PLLA. Unless rapid ECM formation can be achieved before dissolution occurs, PGA hydrolyzes too quickly (t1/2 =16 days) for the purpose of long term meniscal fibrocartilage synthesis. Treatment with chondrogenic or fibrochondrogenic media may induce production of ECM, thus making the culture systems described here more feasible for meniscal tissue engineering.

Conclusion:

In conclusion, we reject the null hypothesis; dynamic cell seeding and culture, as well as increased culture duration, increased scaffold cellularity. Scaffold type also affected cellularity; for bioreactor culture, PGA had higher cell counts versus OPLA, while OPLA had higher cell counts versus PGA in static culture. Cells could only grow unevenly in the pores of the OPLA sponge, and cells could not adhere to the PLLA coating of PGA scaffolds. Increasing the concentration of PLLA coating on a PGA scaffold decreased the cellularity of the scaffold, and did not prevent scaffold dissolution. While PGA culture in a bioreactor produced measureable GAG, no culture technique produced visible collagen. For this reason, and due to the dissolution of PGA scaffolds, the exact culture of conditions described here are not recommended for inducing equine fibrochondrogenesis towards meniscal tissue engineering. Further research is

recommended to enhance extracellular matrix production through additional biomechanical and biological stimulation, including treatment with chondrogenic media, increased culture duration, and increased cell seeding concentrations.

This study was funded by the Comparative Orthopedic Laboratory, University of Missouri. The authors have no conflicts of interest to disclose.

References

Amin M, Kurosaki M, Watanabe T, Tanaka S, and Hori T. 2000. A comparative study of MIB-1 staining indices of gliomas measured by NIH Image analysis program and conventional manual cell counting method. ***Neurologic Research*** **22:495-500.**

Arnoczky SP and Warren RF. 1983. The microvasculature of the meniscus and its response to injury. An experimental study in the dog. ***Am J Sports Med*** **11:131-141.**

AufderHeide AC and Athanasiou KA. 2004. Mechanical stimulation toward tissue engineering of the knee meniscus. ***Ann Biomed Eng*** **32:1161-1174.**

Aufderheide AC and Athanasiou KA. 2005. Comparison of scaffolds and culture conditions for tissue engineering of the knee meniscus. ***Tissue Eng*** **11:1095-1104.**

Beatty MW, Ojha AK, Cook JL, Alberts LR, Mahanna GK, Iwasaki LR, and Nickel JC. 2002. Small intestinal submucosa versus salt-extracted polyglycolic acid-poly-L-lactic acid: a comparison of neocartilage formed in two scaffold materials. ***Tissue Eng*** **8:955-968.**

Benjamin M and Ralphs JR. 1998. Fibrocartilage in tendons and ligaments--an adaptation to compressive load. ***J Anat*** **193 (Pt 4):481-494.**

Benzinou A, Hojeij Y, and Roudot A. 2005. Digital image analysis of haematopoietic clusters. ***Computational Methods and Programs in Biomedicine*** **77:121-127.**

Bilgen B, Ren Y, Pei M, Aaron RK, Ciombor DM. 2009. CD14-negative isolation enhances chondrogenesis in synovial fibroblasts. Tissue Engineering. Part A. 15:3261–3270.

Bilodeau K, and Mantovani D. 2006. Bioreactors for Tissue Engineering: Focus on Mechanical Constraints. A Comparative Review. ***Tissue Eng*****12:2367-83.**

Burks RT, Metcalf MH, and Metcalf RW. 1997. Fifteen-year follow-up of arthroscopic partial meniscectomy. *Arthroscopy* 13:673-679.

Cisa J, Basora J, Madarnas P, Ghibely A, and Navarro-Quilis A. 1995. Meniscal repair by synovial flap transfer. Healing of the avascular zone in rabbits. *Acta Orthop Scand* 66:38-40.

Clark CR, and Ogden JA. 1983. Development of the menisci of the human knee joint. Morphological changes and their potential role in childhood meniscal injury. *J Bone Joint Surg Am* 65:538-547.

Cox JS, Nye CE, Schaefer WW, and Woodstein IJ. 1975. The degenerative effects of partial and total resection of the medial meniscus in dogs' knees. *Clin Orthop Relat Res* 109:178-183.

Davisson T, Sah R, and Ratcliffe A. 1999. Perfusion increases cell content and matrix synthesis in chondrocyte three- dimensional cultures. *Tissue Eng* 8:807-816.

Day R, Boccaccini A, and Shurey A. 2004. Assessment of polyglycolic acid mesh and bioactive glass for soft tissue engineering scaffolds. *Biomaterials* 25:5857-5864.

De Bari C, Dell'Accio F, Tylzanowski P, and Luyten FP. 2001. Multipotent mesenchymal stem cells from adult human synovial membrane. *Arthritis Rheum* 44:1928-1942.

Esposito AR, Moda M, Cattani SM, de Santana GM, Barbieri JA, Munhoz MM, Cardoso TP, Barbo ML, Russo T, D'Amora U. 2013. PLDLA/PCL-T Scaffold for Meniscus Tissue Engineering. *Biores Open Access* 2:138-147.

Farndale RW, Buttle DJ, and Barrett AJ. 1986. Improved quantitation and discrimination of sulphated glycosaminoglycans by use of dimethylmethylene blue. *Biochim Biophys Acta* 883:173-177.

Fithian DC, Kelly MA, and Mow VC. 1990. Material properties and structure-function relationships in the menisci. *Clin Orthop Relat Res* 252:19-31.

Fox DB, Warnock JJ, Stoker AM, Luther JK, and Cockrell M. 2010. Effects of growth factors on equine synovial fibroblasts seeded on synthetic scaffolds for avascular meniscal tissue engineering. *Res Vet Sci* 88:326-32.

Garner P. 2000. Molecular basis and clinical use of biochemical markers of bone, and synovium in joint disease. *Arthritis and Rheumatism* 43:953.

Girman P, Kriz J, Friedmansky J, and Saudek F. 2003. Digital imaging as a possible approach in evaluation of islet yield. *Cell Transplantation* 12:129-133.

Goedkoop A, Rie Md, Teunissen M. 2005. Digital image analysis for the evaluation of the inflammatory infiltrate in psoriasis. *Archives of Dermatological Research* 297:51-59.

Gooch KJ, Kwon JH, Blunk T, Langer R, Freed LE, and Vunjak-Novakovic G. 2001. Effects of mixing intensity on tissue-engineered cartilage. *Biotechnol Bioeng* 72:402-407.

463 **Griffon D, Sedighi M, Sendemir-Urkmez A. 2005. Evaluation of vacuum and dynamic cell**
464 **seeding of polyglycolic acid and chitosan scaffolds for cartilage engineering.**
465 ***American Journal of Veterinary Research* 66:599-605.**

466 **Gunja NJ, and Athanasiou KA. 2010. Additive and synergistic effects of bFGF and hypoxia**
467 **on leporine meniscus cell-seeded PLLA scaffolds. *J Tissue Eng Regen Med* 4:115-122.**

468 **Gurdon JB, Lemaire P, and Kato K. 1993. Community effects and related phenomena in**
469 **development. *Cell* 75:831-834.**

470 **Hee CK, Jonikas MA, and Nicoll SB. 2006. Influence of three-dimensional scaffold on the**
471 **expression of osteogenic differentiation markers by human dermal fibroblasts.**
472 ***Biomaterials* 27:875-884.**

473 **Hu J and Athanasiou K. 2005. Low density cultures of bovine chondrocytes: effects of**
474 **scaffold material and culture system. Biomaterials 26:2001-2012.**

475 **Huey DJ, and Athanasiou KA. 2011. Maturational growth of self-assembled, functional**
476 **menisci as a result of TGF-beta1 and enzymatic chondroitinase-ABC stimulation.**
477 ***Biomaterials* 32:2052-2058.**

478 **Imler SM, Doshi AN, and Levenston ME. 2004. Combined effects of growth factors and**
479 **static mechanical compression on meniscus explant biosynthesis. *Osteoarthritis***
480 ***Cartilage* 12:736-744.**

481 **Ionescu LC, and Mauck RL. 2013. Porosity and cell preseeding influence electrospun**
482 **scaffold maturation and meniscus integration in vitro. *Tissue Eng Part A* 19:538-547.**

483 **Kambic HE, and McDevitt CA. 2005. Spatial organization of types I and II collagen in the**
484 **canine meniscus. *J Orthop Res* 23:142-149.**

485 **Kang SW, Son SM, Lee JS, Lee ES, Lee KY, Park SG, Park JH, and Kim BS. 2006.**
486 **Regeneration of whole meniscus using meniscal cells and polymer scaffolds in a**
487 **rabbit total meniscectomy model. *J Biomed Mater Res A* 77:659-671.**

488 **Kim B, Putnam A, Kulik J. 1998. Optimizing seeding and culture methods to engineer**
489 **smooth muscle tissue on biodegradable polymer matricies. *Biotechnology and***
490 ***Bioengineering* 57:46-54.**

491 **Kobayashi K, Fujimoto E, Deie M, Sumen Y, Ikuta Y, and Ochi M. 2004. Regional**
492 **differences in the healing potential of the meniscus-an organ culture model to**
493 **eliminate the influence of microvasculature and the synovium. *Knee* 11:271-278.**

494 **Kobuna Y, Shirakura K, and Niijima M. 1995. Meniscal repair using a flap of synovium. An**
495 **experimental study in the dog. *Am J Knee Surg* 8:52-55.**

496 **Lavik E, Teng YD, Snyder E, and Langer R. 2002. Seeding neural stem cells on scaffolds of**
497 **PGA, PLA, and their copolymers. *Methods Mol Biol* 198:89-97.**

498 **Levick JR, Price FM, Mason FM. 1996. *Synovial matrix—synovial fluild systems of joints.***
499 **In: WD Comper (ed): Extracellular Matrix. Amsterdam: Harwood Academic**
500 **Publishers, 235-252.**

501 **Loukas CG, Wilson GD, Vojnovic B, and Linney A. 2003. An image analysis-based**
502 **approach for automated counting of cancer cell nuclei in tissue sections. *Cytometry A***
503 **55:30-42.**

504 **Mahmoudifar N, Doran P. 2005. Tissue engineering human cartilage in bioreactors using**
505 **single and composite cell seeded scaffolds. *Biotechnology and Bioengineering* 91:338-**
506 **355.**

507 **Mahmoudifar N, Sikavistas V, Bancroif G, and Mikko A. 2002. Formation of three**
508 **dimensional cell/ polymer constructs for bone tissue engineering in a spinner flask**
509 **and a rotating wall vessel bioreactor. *Journal of Bimedical Material Research* 62:136-**
510 **148.**

511 **Mauck RL, Seyhan SL, Ateshian GA, and Hung CT. 2002. Influence of seeding density and**
512 **dynamic deformational loading on the developing structure/function relationships of**
513 **chondrocyte-seeded agarose hydrogels. *Ann Biomed Eng* 30:1046-1056.**

514 **Moran J, Pazzano B, and Bonassar L. 2003. Characterization of polylactic acid –**
515 **polyglycolic acid composites for cartilage tissue engineering. *Tissue Eng* 9:63-70.**

516 **Mueller SM, Shortkroff S, Schneider TO, Breinan HA, Yannas IV, and Spector M. 1999.**
517 **Meniscus cells seeded in type I and type II collagen-GAG matrices in vitro.**
518 ***Biomaterials* 20:701-709.**

519 **Narita A, Takahara M, Ogino T, Fukushima S, Kimura Y, and Tabata Y. 2009. Effect of**
520 **gelatin hydrogel incorporating fibroblast growth factor 2 on human meniscal cells in**
521 **an organ culture model. *Knee* 16:285-289.**

522 **Nishimura K, Solchaga LA, Caplan AI, Yoo JU, Goldberg VM, and Johnstone B. 1999.**
523 **Chondroprogenitor cells of synovial tissue. *Arthritis Rheum* 42:2631-2637.**

524 **Ochi M, Mochizuki Y, Deie M, and Ikuta Y. 1996. Augmented meniscal healing with free**
525 **synovial autografts: an organ culture model. *Arch Orthop Trauma Surg* 115:123-126.**

526 **Pazzano D, Davisson T, Seidel J, Pei M, GrayM. 2004. Long term culture of tissue**
527 **engineered cartilage in a perfused chamber with mechanical stimulation.**
528 ***Biorheology* 41:445-458.**

Pazzano D, Mercier K, Moran J. 2000. Comparison of chondrogenensis in static and perfused bioreactor culture. *Biotechnology Progress* 16:893-896.

Pei M, He F, and Vunjak-Novakovic G. 2008. Synovium-derived stem cell-based chondrogenesis. *Differentiation* 76:1044-1056.

Pei, M., He, F., Kish, V.L., Vunjak-Novakovic, G. 2008. Engineering of functional cartilage tissue using stem cells from synovial lining: a preliminary study. Clinical Orthopedics and Related Research 466, 1880-1889.

Peroni JF, and Stick JA. 2002. Evaluation of a cranial arthroscopic approach to the stifle joint for the treatment of femorotibial joint disease in horses: 23 cases (1998-1999). *J Am Vet Med Assoc* 220:1046-1052.

Reddy GK, and Enwemeka CS. 1996. A simplified method for the analysis of hydroxyproline in biological tissues. *Clin Biochem* 29:225-229.

Rodeo SA, Seneviratne A, Suzuki K, Felker K, Wickiewicz TL, and Warren RF. 2000. Histological analysis of human meniscal allografts. A preliminary report. *J Bone Joint Surg Am* 82-A:1071-1082.

Sakimura K, Matsumoto T, Miyamoto C, Osaki M, and Shindo H. 2006. Effects of insulin-like growth factor I on transforming growth factor beta1 induced chondrogenesis of synovium-derived mesenchymal stem cells cultured in a polyglycolic acid scaffold. *Cells Tissues Organs* 183:55-61.

Sha'ban M, Kim SH, Idrus RB, and Khang G. 2008. Fibrin and poly(lactic-co-glycolic acid) hybrid scaffold promotes early chondrogenesis of articular chondrocytes: an in vitro study. *J Orthop Surg* 3:17.

Sherwood JK, Riley SL, Palazzolo R, Brown SC, Monkhouse DC, Coates M, Griffith LG, Landeen LK, and Ratcliffe A. 2002. A three-dimensional osteochondral composite scaffold for articular cartilage repair. *Biomaterials* 23:4739-4751.

Shirakura K, Niijima M, Kobuna Y, and Kizuki S. 1997. Free synovium promotes meniscal healing. Synovium, muscle and synthetic mesh compared in dogs. *Acta Orthop Scand* 68:51-54.

Smith R, Dunlon B, Gupta, E. 1995. Effects of fluid induced shear on articular chondrocyte morphology and metabolism in vitro. *Journal of Orthopaedic Research* 13:824.

Stading M, and R L. 1999. Mechanical shear properties of cell-polymer cartilage constructs. *Tissue Eng* 5:241-250.

Strober W. 2001. Trypan blue exclusion test of cell viability. *Curr Protoc Immunol* Appendix 3:Appendix 3B.

Tan, Y., Zhang, Y., and Pei, M. 2010. Meniscus reconstruction through coculturing

meniscus cells with synovium-derived stem cells on small intestine submucosa—a pilot study to engineer meniscus tissue constructs. Tissue Eng Part A 16, 67-79.

Valiyaveettil M, Mort JS, and McDevitt CA. 2005. The concentration, gene expression, and spatial distribution of aggrecan in canine articular cartilage, meniscus, and anterior and posterior cruciate ligaments: a new molecular distinction between hyaline cartilage and fibrocartilage in the knee joint. *Connect Tissue Res* 46:83-91.

Vunjak-Novakovic G, Obradovic B, Martin I, Bursac PM, Langer R, and Freed LE. 1998. Dynamic cell seeding of polymer scaffolds for cartilage tissue engineering. *Biotechnol Prog* 14:193-202.

Walmsley JP. 1995. Vertical tears of the cranial horn of the meniscus and its cranial ligament in the equine femorotibial joint: 7 cases and their treatment by arthroscopic surgery. *Equine Vet J* 27:20-25.

Walmsley JR, Phillips TJ, and Townsend HG. 2003. Meniscal tears in horses: an evaluation of clinical signs and arthroscopic treatment of 80 cases. *Equine Vet J* 35:402-406.

Wu F, Dunkelman N, and Peterson A. 1999. Bioreactor development for tissue engineered cartilage. *Annals of the New York Academy of Science* 875:405-411.

Figures

Figure 1. Rotating wall bioreactor flask (110mL) containing media and PGA scaffolds seeded with equine fibroblast-like synoviocytes (**A**). Flasks loaded on the rotating base apparatus; flasks rotate around their longitudinal axis (**B**).

Figure 2. Static culture of equine fibroblast- like synoviocytes on PGA scaffolds in a 24 well tissue culture plate, with each well containing 2mL of supplemented DMEM.

Figure 3. Method for viewing all scaffolds to standardize cell counts and determine regional cell count differences between the scaffold center and periphery. Cells were counted at the periphery and central regions (dark dotted circles) of each scaffold (cross- hatched circle) using digital image analysis; peripheral cell counts (light dotted circles) were obtained at the 2o'clock, 6o'clock and 19o'clock positions. Circles represent a low power (10X objective) field of view.

Figure 4. Scanning electron microscopy of a 2% PLLA coated PGA scaffold (**A**) and a 4% PLLA coated scaffold (**B**) prior to cell seeding; bar = 100µm.

Figure 5. Rotating wall bioreactor flask containing 2% PLLA coated PGA scaffolds, strung on suture to ensure equal submersion and positioning in the rotating flask.

Figure 6. Micrographs of scaffolds seeded with equine fibroblast-like synoviocytes; Hematoxylin and Eosin staining, 10x objective magnification; bar = 100µm. **A**) PGA scaffold cultured in a static environment; **B**) PGA scaffold cultured in a dynamic environment (rotating bioreactor); **C**) OPLA scaffold cultured in a dynamic environment (rotating bioreactor); **D**) OPLA scaffold cultured in a static environment. Note the intact PGA fibers (open arrow) and the cells located in clumps in the pores of the OPLA scaffold (closed arrows).

Figure 7. Mean ±Standard Error of the Mean (SEM) of dsDNA content of PGA scaffolds coated in 2% PLLA and 4% PLLA, seeded dynamically and cultured in a rotating bioreactor for 14 days and 21 days. A bar and (*) indicates a significant difference between two treatment groups($P<0.05$).

Figure 8. Photomicrographs of 2% PLLA coated PGA constructs harvested on day 10, under standard light (column **A**) and under laser confocal microscopy (column **B**), using the calcein AM-ethidium homodimer live-dead assay. Images represent scaffold transverse cross sections (row **T**) and scaffold surface coronal sections (row **C**). Green stained cells are alive, red stained cells are dead. 10x objective magnification; bar = 100µm.

Figure 9. Photomicrographs of 2% PLLA coated PGA constructs harvested on day 21, under standard light (column **A**) and under laser confocal microscopy (column **B**), using the calcein AM-ethidium homodimer live-dead assay. Images represent scaffold transverse cross sections (row **T**) and scaffold surface coronal sections (row **C**). Green stained cells are alive, red stained cells are dead. Note the spurious red staining of scaffold PGA fibers. 10x objective magnification; bar = 100µm.

Figure 10**.** Photomicrographs of 4% PLLA coated PGA constructs harvested on day 10, under standard light (column **A**) and under laser confocal microscopy (column **B**), using the calcein

AM-ethidium homodimer live-dead assay. Images represent scaffold transverse cross sections (row **T**) and scaffold surface coronal sections (row **C**). Green stained cells are alive, red stained cells are dead. Note the spurious red staining of PGA fibers. 10x objective magnification; bar = 100µm.

Figure 11. Photomicrographs of 4% PLLA coated PGA constructs harvested on day 21, under standard light (column **A**) and under laser confocal microscopy (column **B**), using the calcein AM-ethidium homodimer live-dead assay. Images represent scaffold transverse cross sections (row **T**) and scaffold surface coronal sections (row **C**). Green stained cells are alive, red stained cells are dead. Note the spurious red staining of PGA fibers.10x objective magnification; bar = 100µm.

Figure 12. Photomicrographs of 2% PLLA coated PGA scaffolds harvested on day 10 (row **1**) and day 21 (row **2**), and 4% PLLA coated PGA scaffolds harvested on day 10 (row **3**) and day 21 (row **4**), H+E staining. Column **A** represents images of the center of the construct and column **B** represents images taken of the scaffold periphery. Note that the cells have grown in dense clusters; 10x objective magnification; bar = 100µm.

Figure 1

Dynamic culture: rotating bioreactor apparatus.

Rotating wall bioreactor flask (110mL) containing media and PGA scaffolds seeded with equine fibroblast-like synoviocytes (A). Flasks loaded on the rotating base apparatus; flasks rotate around their longitudinal axis (B).

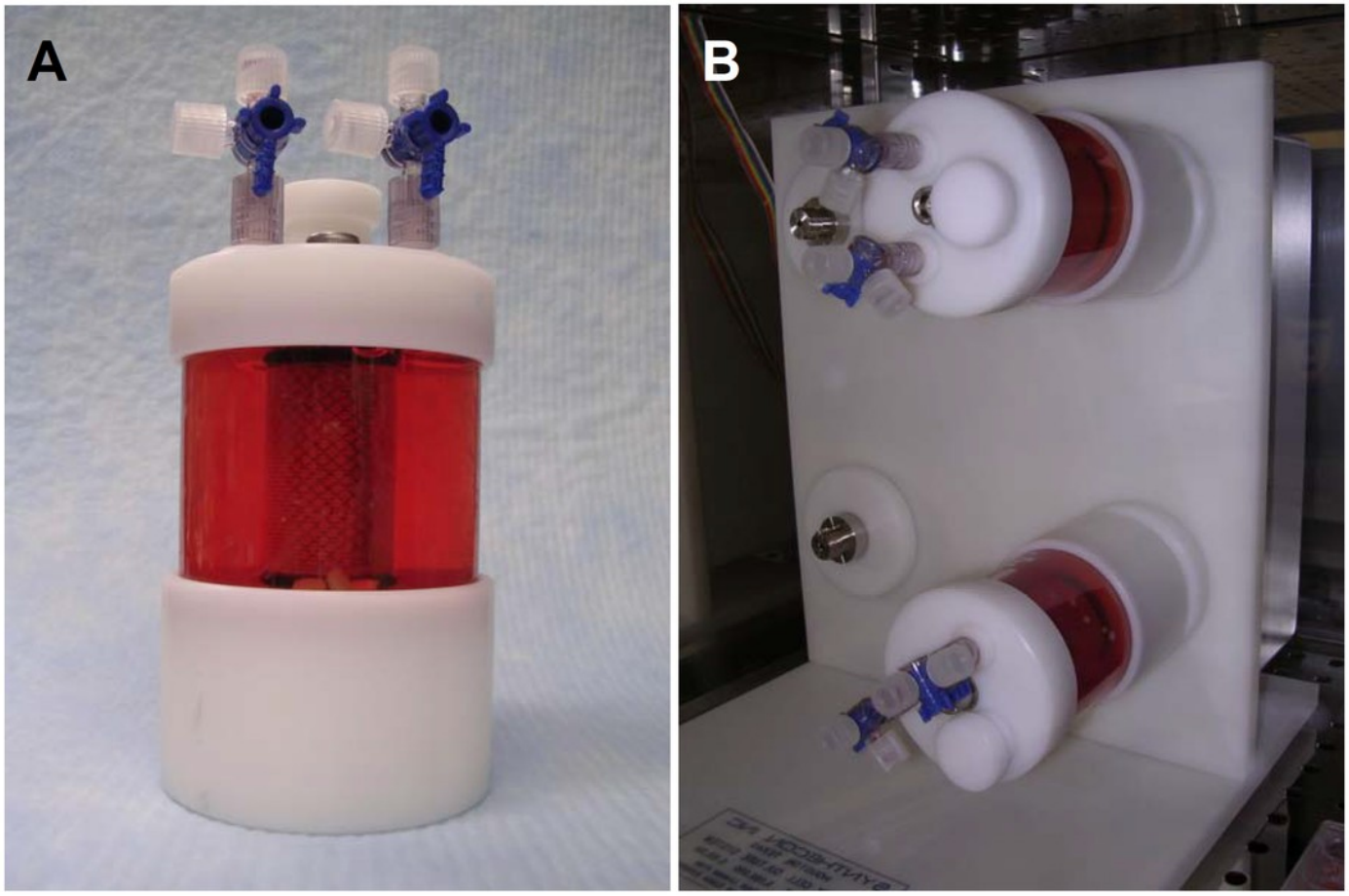

Figure 2

Static culture.

Static culture of equine fibroblast- like synoviocytes on PGA scaffolds in a 24 well tissue culture plate, with each well containing 2mL of supplemented DMEM.

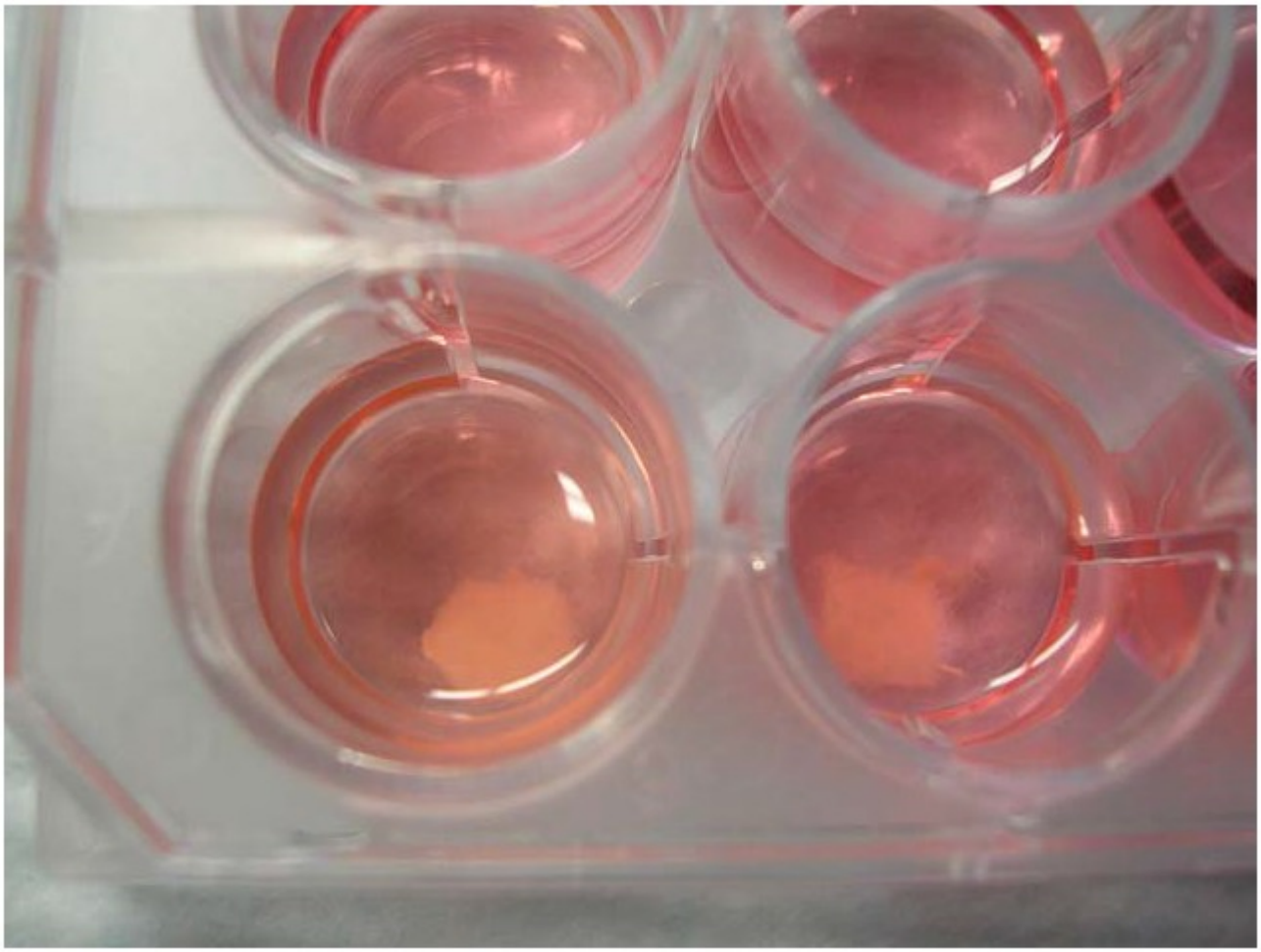

Figure 3

Histologic cell counting method.

Method for viewing all scaffolds to standardize cell counts and determine regional cell count differences between the scaffold center and periphery. Cells were counted at the periphery and central regions (dark dotted circles) of each scaffold (cross- hatched circle) using digital image analysis; peripheral cell counts (light dotted circles) were obtained at the 2o'clock, 6o'clock and 19o'clock positions. Circles represent a low power (10X objective) field of view.

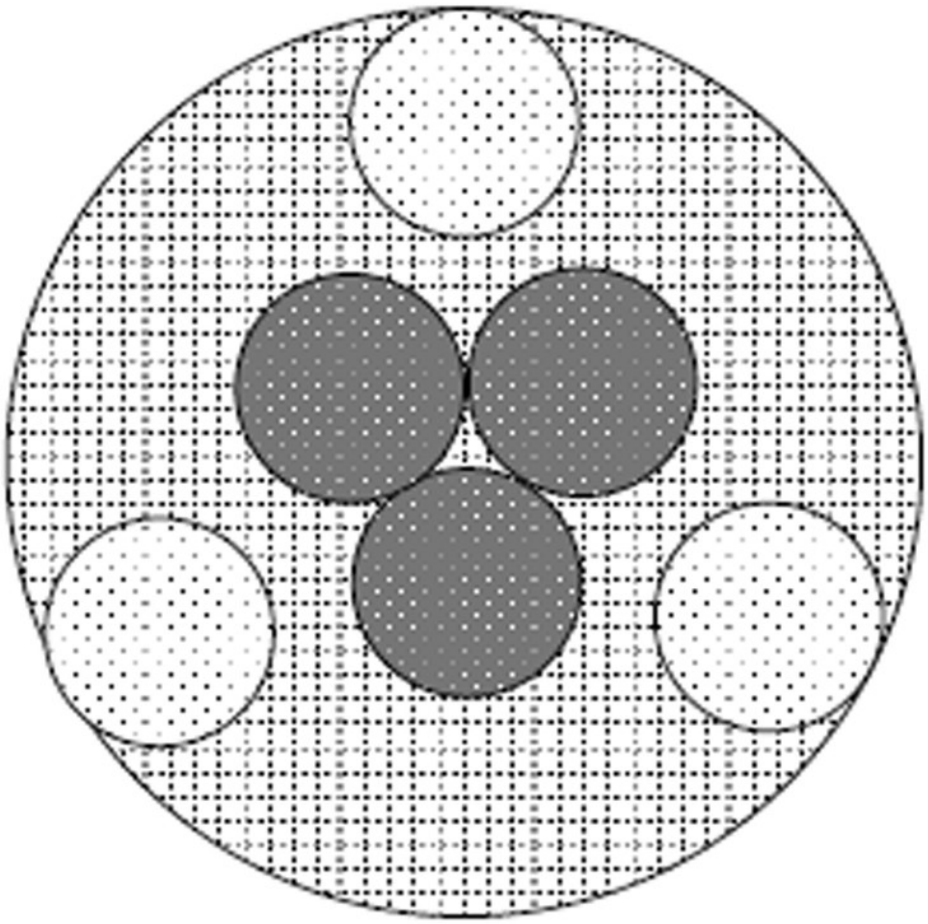

Figure 4

PLLA coated scaffolds.

Scanning electron microscopy of a 2% PLLA coated PGA scaffold (**A**) and a 4% PLLA coated scaffold (**B**) prior to cell seeding; bar = 100µm.

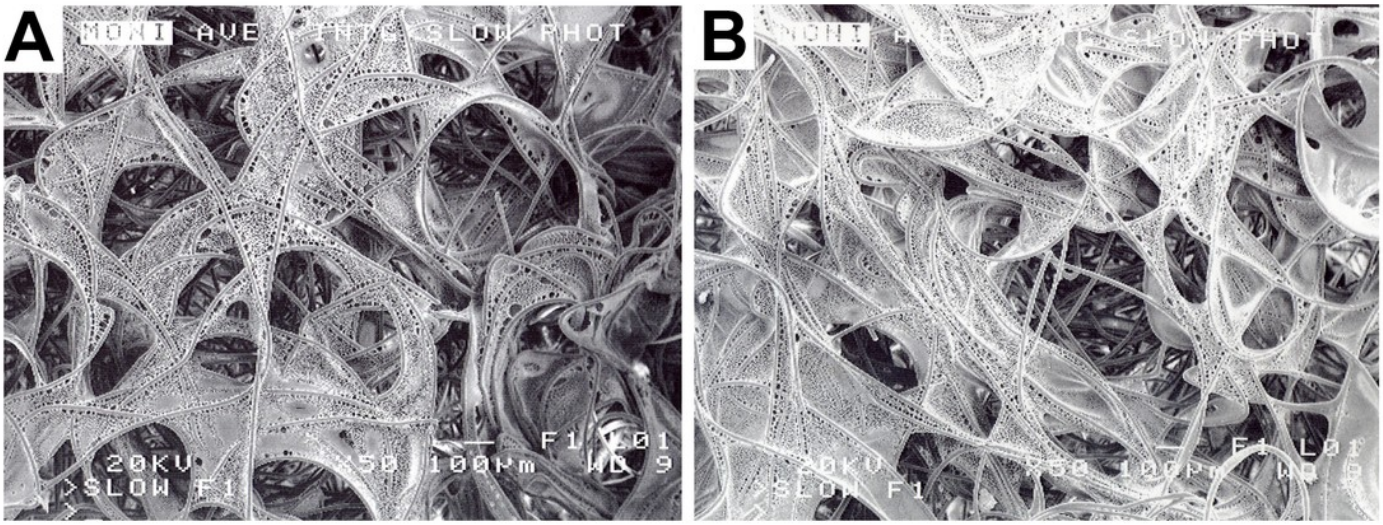

Figure 5

Positioning of PLLA coated scaffolds in the rotating bioreactor.

Rotating wall bioreactor flask containing 2% PLLA coated PGA scaffolds, strung on suture to ensure equal submersion and positioning in the rotating flask.

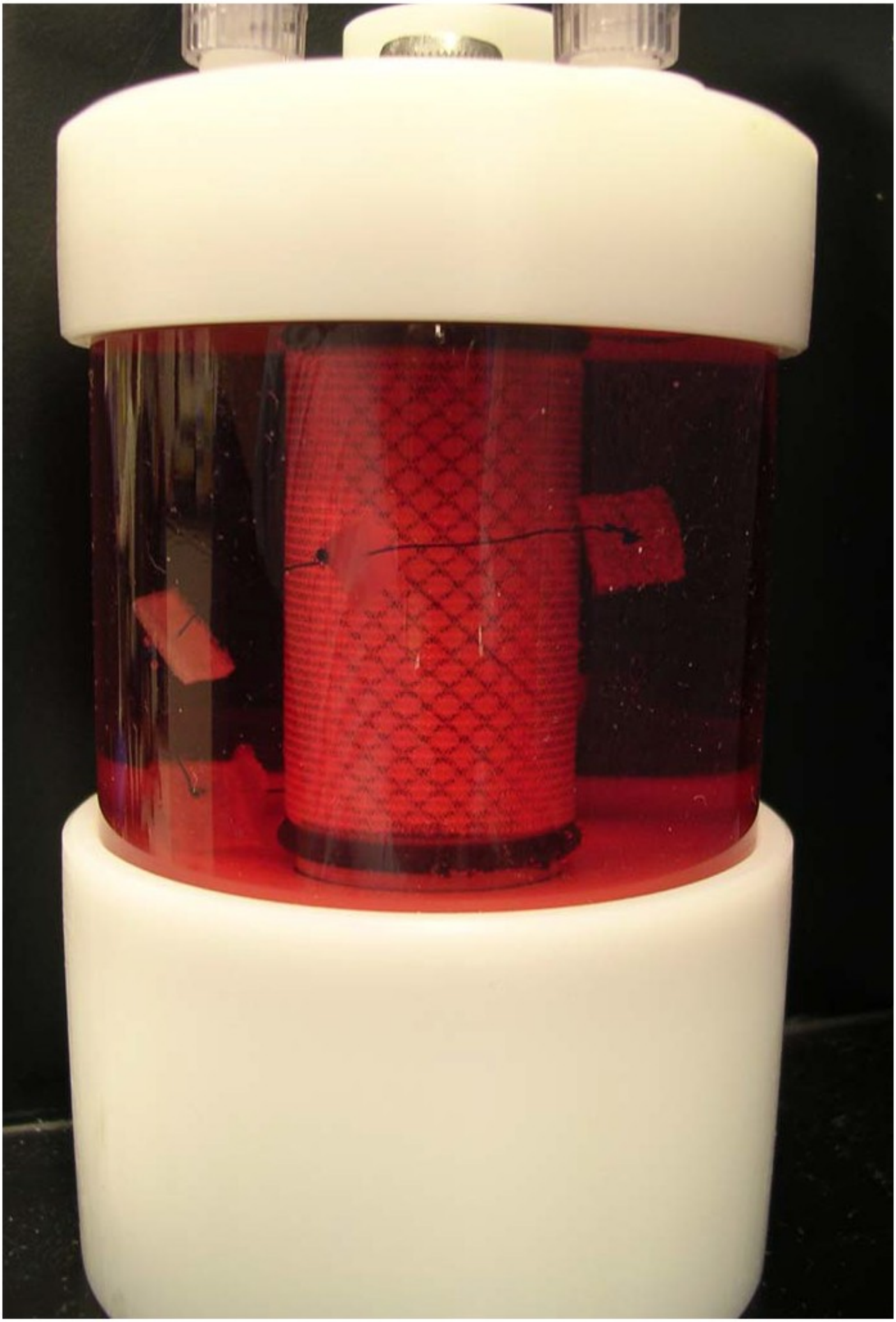

Figure 6

Histologic cell distribution on PGA and OPLA scaffolds.

Micrographs of scaffolds seeded with equine fibroblast-like synoviocytes; Hematoxylin and Eosin staining, 10x objective magnification; bar = 100µm. A) PGA scaffold cultured in a static environment; B) PGA scaffold cultured in a dynamic environment (rotating bioreactor); C) OPLA scaffold cultured in a dynamic environment (rotating bioreactor); D) OPLA scaffold cultured in a static environment. Note the intact PGA fibers (open arrow) and the cells located in clumps in the pores of the OPLA scaffold (closed arrows).

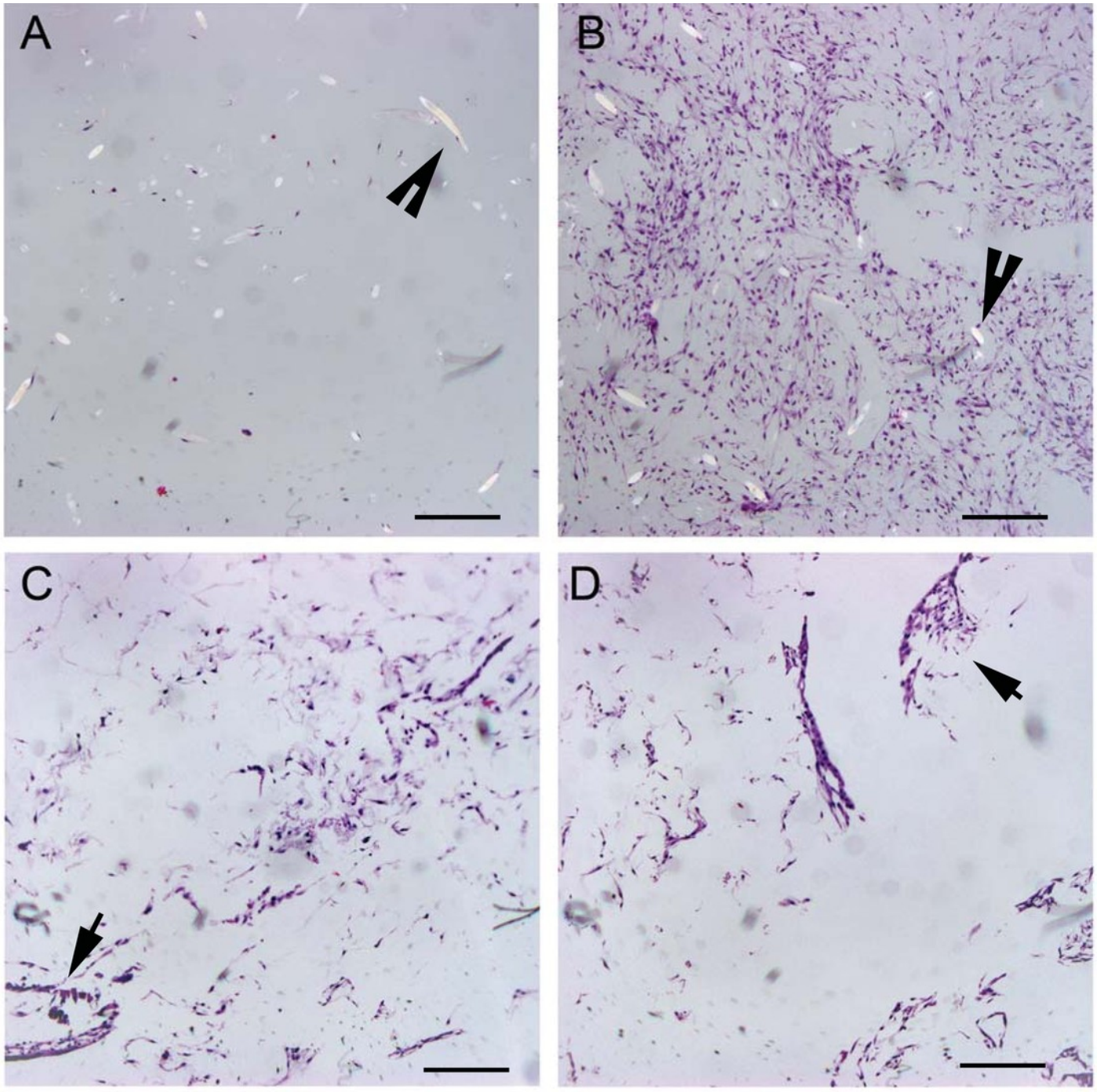

Figure 7

Double stranded DNA content of PLLA coated scaffolds.

Mean ±Standard Error of the Mean (SEM) of dsDNA content of PGA scaffolds coated in 2% PLLA and 4% PLLA, seeded dynamically and cultured in a rotating bioreactor for 14 days and 21 days. A bar and (*) indicates a significant difference between two treatment groups ($P<0.05$).

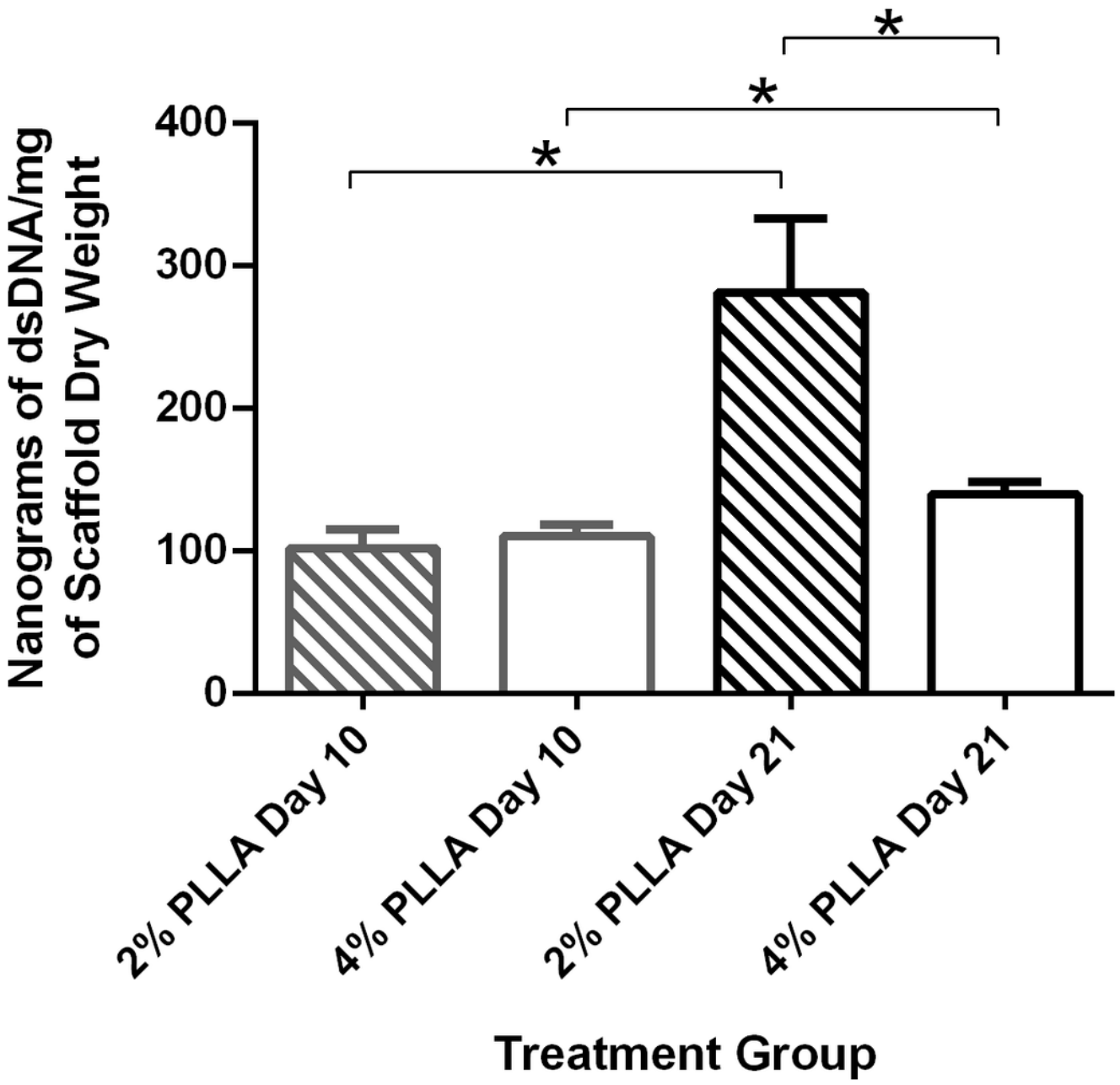

Figure 8

Cell viability: 2% PLLA scaffolds

Photomicrographs of 2% PLLA coated PGA constructs harvested on day 10, under standard light (column **A**) and under laser confocal microscopy (column **B**), using the calcein AM-ethidium homodimer live-dead assay. Images represent scaffold transverse cross sections (row **T**) and scaffold surface coronal sections (row **C**). Green stained cells are alive, red stained cells are dead. 10x objective magnification; bar = 100µm.

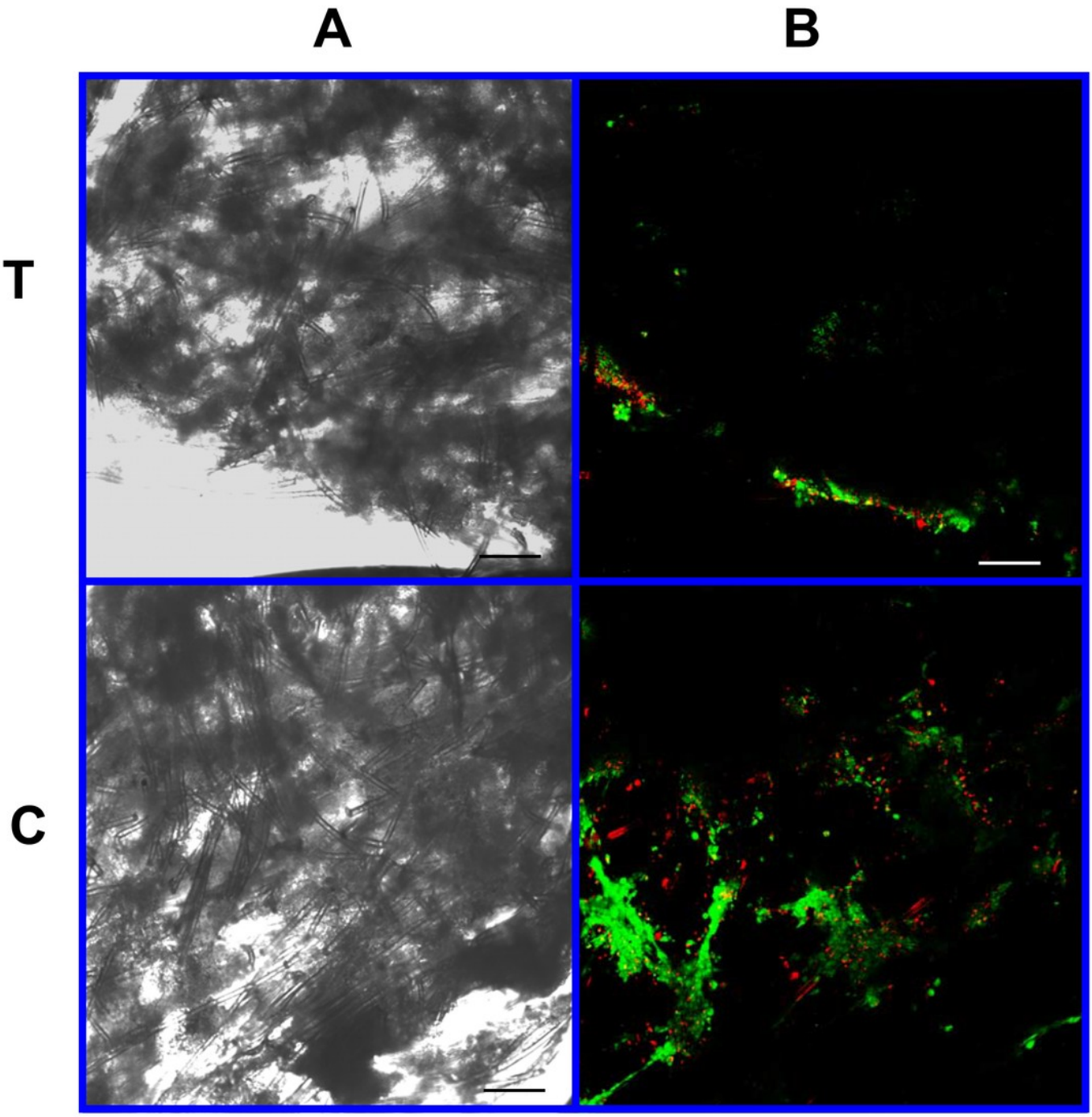

Figure 9

Cell viability: 2% PLLA scaffolds

Photomicrographs of 2% PLLA coated PGA constructs harvested on day 21, under standard light (column **A**) and under laser confocal microscopy (column **B**), using the calcein AM-ethidium homodimer live-dead assay. Images represent scaffold transverse cross sections (row **T**) and scaffold surface coronal sections (row **C**). Green stained cells are alive, red stained cells are dead. Note the spurious red staining of scaffold PGA fibers. 10x objective magnification; bar = 100µm.

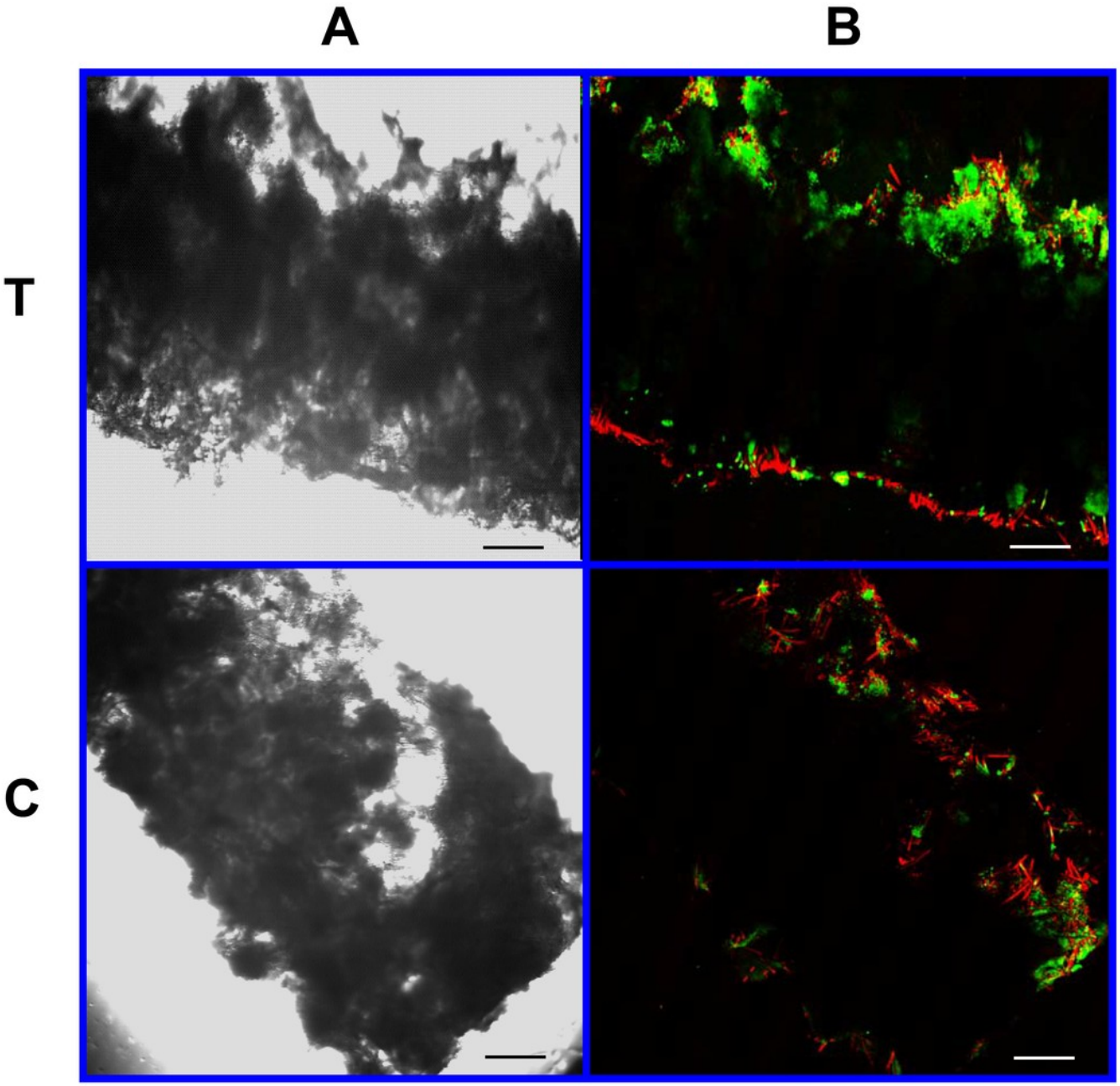

Figure 10

Cell viability assay: 4% PLLA scaffolds

Photomicrographs of 4% PLLA coated PGA constructs harvested on day 10, under standard light (column **A**) and under laser confocal microscopy (column **B**), using the calcein AM-ethidium homodimer live-dead assay. Images represent scaffold transverse cross sections (row **T**) and scaffold surface coronal sections (row **C**). Green stained cells are alive, red stained cells are dead. Note the spurious red staining of PGA fibers. 10x objective magnification; bar = 100µm.

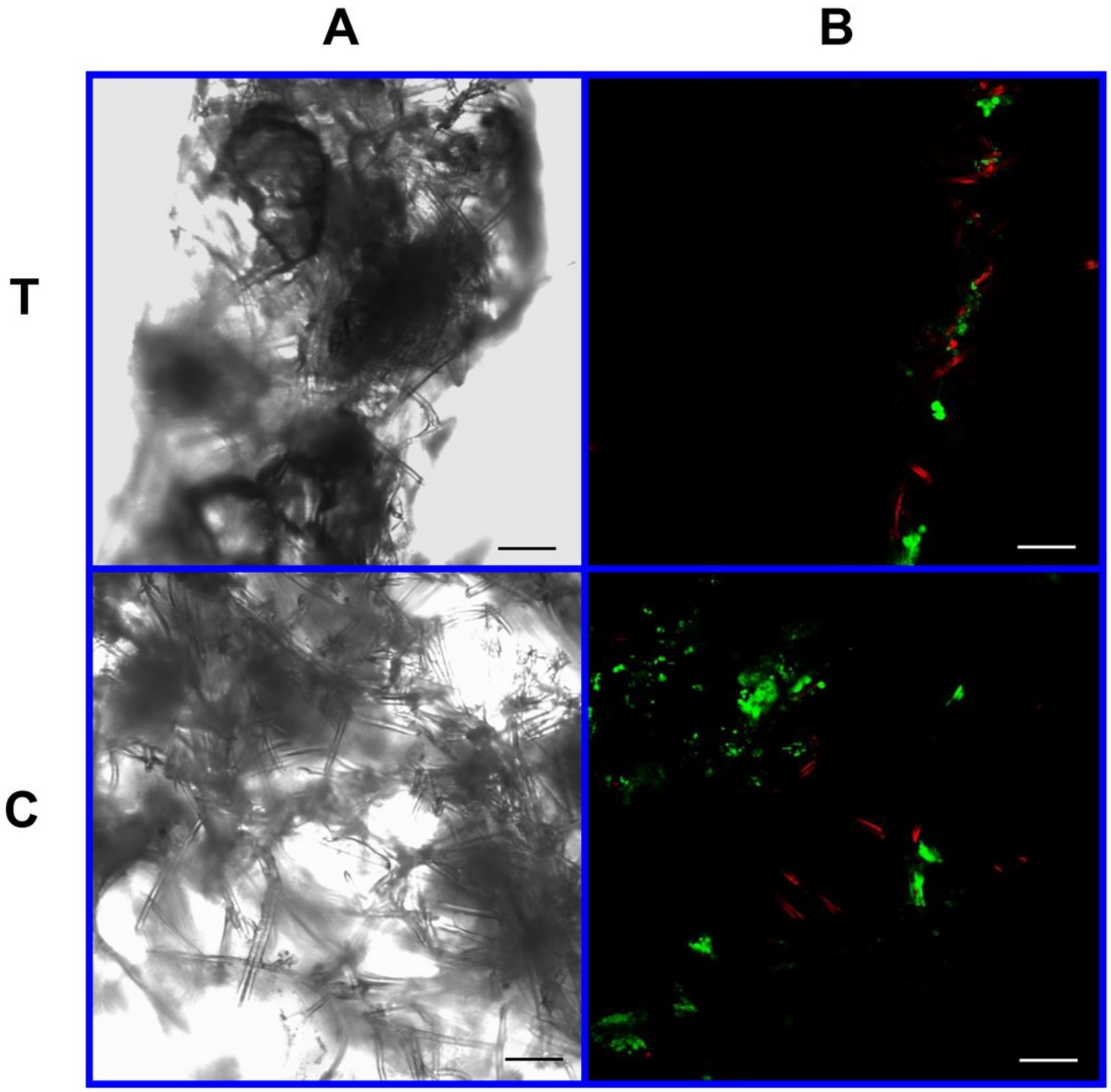

Figure 11

Cell viability: 4% PLLA scaffolds

Photomicrographs of 4% PLLA coated PGA constructs harvested on day 21, under standard light (column **A**) and under laser confocal microscopy (column **B**), using the calcein AM-ethidium homodimer live-dead assay. Images represent scaffold transverse cross sections (row T) and scaffold surface coronal sections (row **C**). Green stained cells are alive, red stained cells are dead. Note the spurious red staining of PGA fibers.10x objective magnification; bar = 100µm.

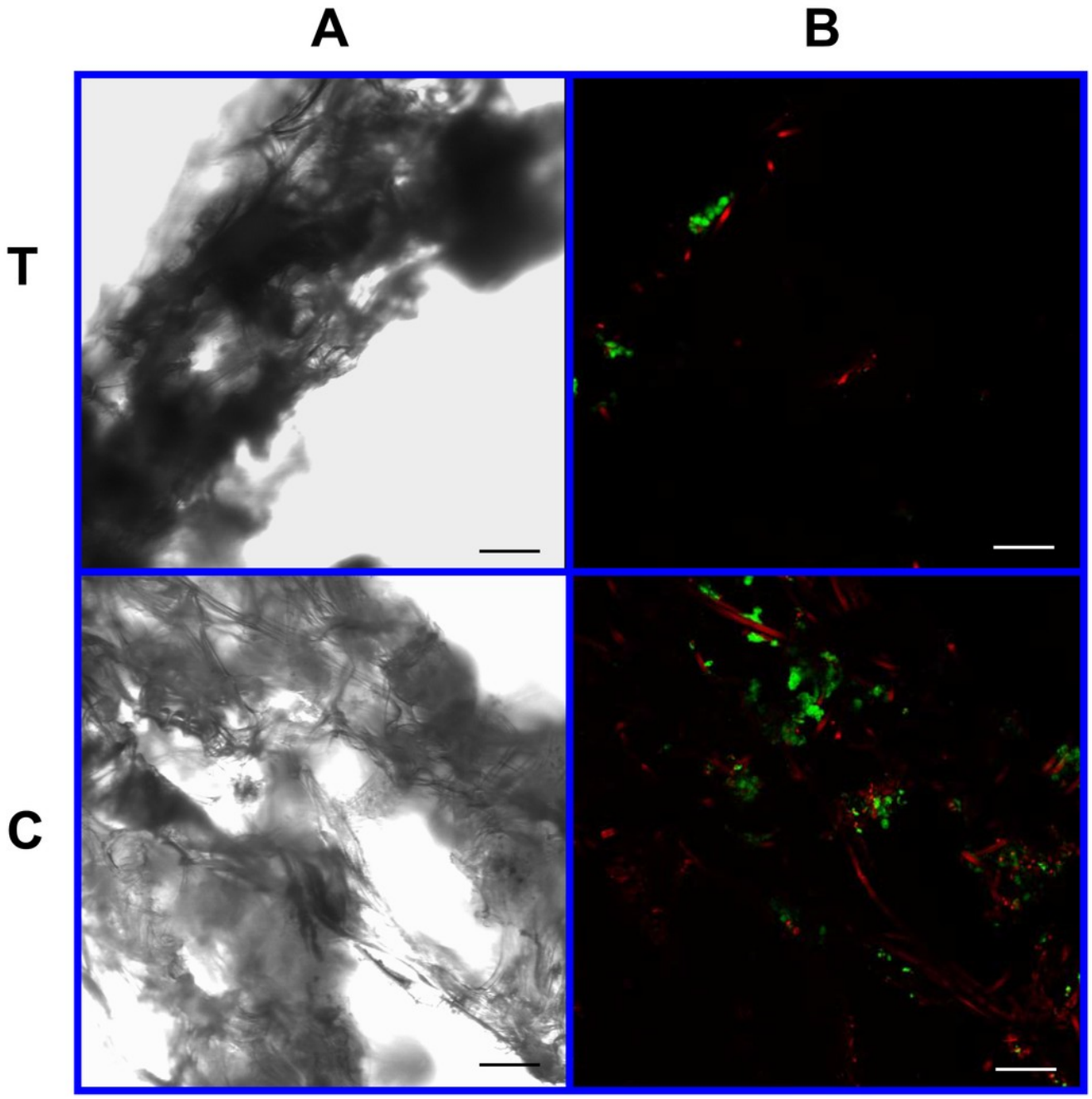

Figure 12

Distribution of cells on 2% and 4% PLLA coated PGA scaffolds

Figure 12. Photomicrographs of 2% PLLA coated PGA scaffolds harvested on day 10 (row **1**) and day 21 (row **2)**, and 4% PLLA coated PGA scaffolds harvested on day 10 (row **3**) and day 21 (row **4**), H+E staining. Column **A** represents images of the center of the construct and column **B** represents images taken of the scaffold periphery. Note that the cells have grown in dense clusters; 10x objective magnification; bar = 100µm.

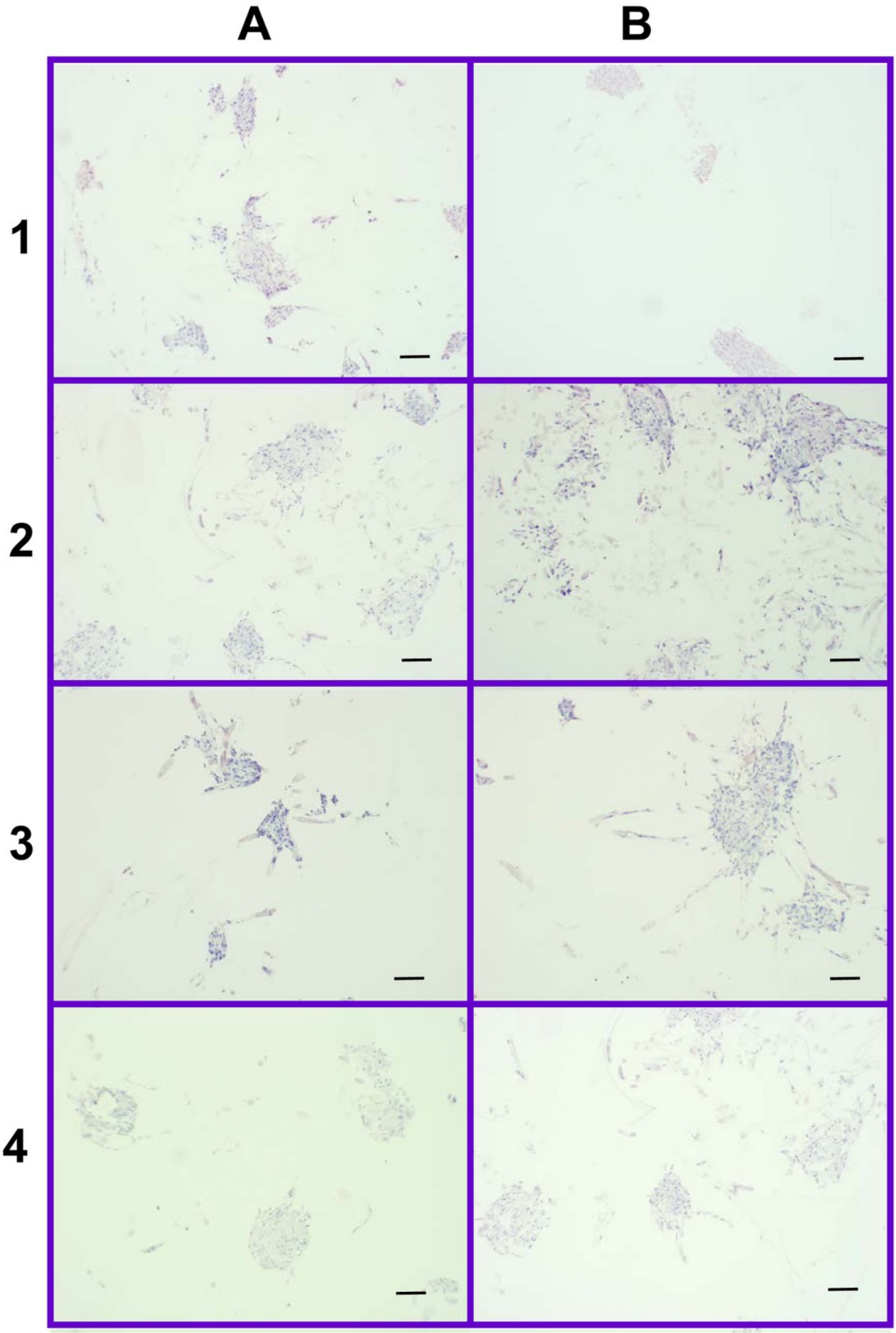

Table 1(on next page)

The effect of seeding and cell culture biomechanical environment and the effect of scaffold type on scaffold cellularity.

	Cell Count (Mean number of cells per 10x objective field ±SD)		Effect of biomechanical environment (dynamic vs static culture)
Scaffold type:	Biomechanical environment:		
	Dynamic culture	Static culture	
PGA	1128 ±575 cells	54 ±34 cells	P<0.001
OPLA	375 ±118 cells	301 ±65 cells	P= 0.028
Effect of scaffold type (PGA vs OPLA)	P=0.017	P=0.0217	

Table 2(on next page)

Peripheral and central cell count (Mean number of cells per 10x objective field ±SD).

Scaffold	Peripheral cell count	Central cell count	P- value
PGA-D	1433 ±487	724 ±314	P<0.001
PGA-S	80 ±28	28 ±11	P<0.001
OPLA-D	476 ±90	295 ±55	P<0.001